Published in final edited form as:
J Pain Symptom Manage. 2008 September ; 36(3): 289–303. doi:10.1016/j.jpainsymman.2007.10.005.

Intravenous Ibandronate Rapidly Reduces Pain, Neurochemical Indices of Central Sensitization, Tumor Burden, and Skeletal Destruction in a Mouse Model of Bone Cancer

Kyle G. Halvorson, BA, **Molly A. Sevcik, BA**, **Joseph R. Ghilardi, BS, BA**, **Lucy J. Sullivan, BA**, **Nathan J. Koewler, BS**, **Frieder Bauss, PhD**, and **Patrick W. Mantyh, PhD**
Neurosystems Center and Departments of Diagnostic and Biological Sciences, Psychiatry, Neuroscience, and Cancer Center, University of Minnesota (K.G.H., M.A.S., L.J.S., N.J.K.), and Research Service, VA Medical Center (J.R.G.), Minneapolis, Minnesota, USA; Roche Diagnostics GmbH, Pharma Research Penzberg (F.B.), Penzberg, Germany; and Department of Pharmacology (P.W.M.), University of Arizona College of Medicine, Tucson, Arizona, USA

Abstract

Over half of all chronic cancer pain arises from metastases to bone and bone cancer pain is one of the most difficult of all persistent pain states to fully control. Currently, bone pain is treated primarily by opioid-based therapies, which are frequently accompanied by significant unwanted side effects. In an effort to develop non-opioid-based therapies that could rapidly attenuate tumor-induced bone pain, we examined the effect of intravenous administration of the bisphosphonate, ibandronate, in a mouse model of bone cancer pain. Following injection and confinement of green fluorescent protein-transfected murine osteolytic 2472 sarcoma cells into the marrow space of the femur of male C3H/HeJ mice, ibandronate was administered either as a single dose (300 μg/kg), at day 7 post-tumor injection, when tumor-induced bone destruction and pain were first evident, or in three consecutive doses (100 μg/kg/day) at day 7, 8 and 9 post-tumor injection. Intravenous ibandronate administered once or in three consecutive doses reduced ongoing and movement-evoked bone cancer pain-related behaviors, neurochemical markers of central sensitization, tumor burden and tumor-induced bone destruction. These results support limited clinical trials that suggest the potential of ibandronate to rapidly attenuate bone pain and illuminate the mechanisms that may be responsible for limiting pain and disease progression.

Keywords

Tumor bone pain; skeletal malignancies; bisphosphonates; ibandronate; nociception

Introduction

The most frequent presenting symptom of tumor metastasis to the skeleton is bone pain. Pain originating from skeletal metastases usually increases in intensity with the evolution of the disease and is commonly divided into three categories: ongoing pain, spontaneous

Address correspondence to: Patrick W. Mantyh, PhD, Department of Pharmacology, University of Arizona College of Medicine, 1501 Campbell Avenue, Tucson, AZ 85724, USA, E-mail: pmantyh@email.arizona.edu.

breakthrough (incident) pain, and movement-evoked breakthrough pain.[1, 2] Ongoing pain, which is the most frequent initial symptom of bone cancer, begins as a dull, constant, throbbing pain that increases in intensity with time.[3, 4] As bone cancer progresses, intermittent episodes of extreme pain can occur spontaneously, or more commonly, after weight-bearing or movement of the affected limb.[3, 4] Of these types of pain, breakthrough pain is the most difficult to control, as the dose of opioids required to fully control this pain are generally high and accompanied by significant unwanted side effects, such as somnolence, cognitive impairment, and constipation.[3, 5]

In an effort to identify non-opioid therapies that could attenuate bone cancer pain we focused on the bisphosphonate, ibandronate, as it is highly potent, can be administered orally or intravenously (IV), and has a favorable renal safety profile.[6] A third-generation bisphosphonate, such as ibandronate, displays a high affinity for mineralized bone such that within a few hours following a single subcutaneous or IV administration about 40–60% of the bisphosphonate is incorporated into mineralized bone.[7, 8] Once bound to bone, bisphosphonates are internalized by the osteoclasts during the bone resorption process. This is followed by a subsequent induction of apoptosis by two different modes of action. They either form cytotoxic metabolites (non-nitrogen-containing bisphosphonates, such as etidronate or clodronate) or inhibit protein tyrosine phosphatases (nitrogen-containing bisphosphonates, such as alendronate, risedronate or ibandronate).[9,10] In animals or humans that receive chronic bisphosphonate treatment, the concentration of bisphosphonate at the mineralized bone/osteoclast interface has been estimated to be in the order of 10^{-4} M to 10^{-3} M.[11] The final concentration depends on the dose, potency and duration of treatment of the respective bisphosphonate, and on the underlying disease.

In light of the severity and frequency of bone pain and the relatively limited therapeutic options to rapidly reduce this pain, bisphosphonate therapy has been incorporated into clinical practice based on observation and a few trials. For example, IV infusion of ibandronate in patients with metastatic bone pain due to breast cancer was reported to induce rapid and significant reduction in pain.[12] However, what remains unclear is what specific sites in the bone or related nociceptive systems are influenced by ibandronate infusion.

In the present report, we explore whether this clinical observation can be appropriately simulated in an *in vivo* model of bone cancer pain by IV infusion of ibandronate, and thereby gain insight into the underlying mechanisms. In these experiments, we used a mouse model, in which osteolytic murine sarcoma cells, stably transfected with green fluorescent protein (GFP), are injected and confined to the marrow space of the mouse femur.[13, 14] As the tumor cells are injected directly into the femur and the injection site sealed with dental grade amalgam to prevent escape of tumor cells, the cells are confined to the femur without the confound of extensive tumor growth outside the bone. We show that within days of either single or multiple IV infusions of ibandronate, there was significant attenuation of both movement-evoked and spontaneous bone cancer pain, markers of central sensitization, tumor-induced bone destruction and tumor burden.

Methods

Animals

Experiments were performed on a total of 91 adult male C3H/HeJ mice (Jackson Laboratories, Bar Harbor, Maine, USA), weighing 20–25g. The mice were housed in accordance with the National Institutes of Health guidelines under specific pathogen free (SPF) conditions in autoclaved cages maintained at 22°C with a 12-hour alternating light and dark cycle and were given autoclaved food and water ad libitum. All procedures were approved by the Institutional Animal Care and Use Committee at the University of Minnesota.

Culture and Injection of Tumor Cells

Osteolytic murine sarcoma cells were obtained (NCTC 2472, ATCC, Rockville, Maryland, USA), stably transfected with green fluorescent protein (GFP), and maintained as previously described.[15] Following induction of general anesthesia with ketamine:xylazine (75 mg/kg, intramuscularly), an arthrotomy was performed exposing the condyles of the distal femur. The bone was cored with a 30 gauge needle inserted at the level of the intercondylar notch. The coring needle was then replaced with a 29 gauge hypodermic needle (Terumo Medical Corporation, Elkton, Maryland, USA), used to inject either Hank's buffered sterile saline as the control (HBSS, Sigma, St. Louis, Missouri, USA; 20μl; sham, *n*=20) or HBSS containing 10^5 sarcoma cells (20μl; sarcoma, *n*=71) into the intramedullary space. In order to prevent cell reflux following injection, the injection site was sealed with dental grade amalgam (Dentsply, Milford, Delaware, USA), using an endodontic Messing gun (Union Broach, Emigsville, Pennsylvania, USA), followed by copious irrigation with sterile filtered water (hypotonic solution). Wound closure was achieved using a single 7mm auto wound clip (Becton Dickinson, Sparks, Maryland, USA). Animals injected with sarcoma cells were further divided into two groups, one group euthanized and processed at day 10 post-tumor injection (n = 39) and the other second group at day 14 post-tumor injection (n = 32). A day 10 endpoint was selected from one group of animals to more accurately quantify bone destruction and tumor proliferation in the sarcoma + vehicle and sarcoma + ibandronate animals. The day 14 endpoint was used as the time point of maximal expression of cancer-related pain behaviors and changes in expression of neurochemical markers of peripheral and central sensitization. Sham animals were used for control analysis of neurochemical changes and bone histology as they have previously been shown not to be significantly different behaviorally, neurochemically, or histologically from naïve animals.[16, 17]

Treatment with Ibandronate

Mice were randomly placed into three treatment groups receiving either sterile saline (sham + vehicle: *n*=20; sarcoma + vehicle: *n*=24; 5 ml/kg IV, given as a 10sec administration), the bisphosphonate, ibandronate, on three consecutive days (sarcoma + ibandronate: *n*=33, 100 μg/kg/d IV, from Roche Diagnostics GmbH, Penzberg, Germany), or ibandronate as a single dose (sarcoma + ibandronate: *n*=5, 300 μg/kg IV). Treatment was initiated at day 7 following tumor cell or sham inoculation which is based on the time at which observable bone destruction begins[14] and was terminated at either day 10 or day 14 post-injection for consecutive dosing or day 14 post-injection for the single dose.

Characterization of Study Medication

In vivo, ibandronate is 2-, 10-, 50- and 500-fold more potent at inhibiting bone resorption than risedronate, alendronate, pamidronate and clodronate, respectively.[18] Ibandronate can, therefore, be used at lower doses than most bisphosphonates.

Consistent with other bisphosphonates,[8] preclinical data show that ibandronate distributes rapidly and concentrates predominantly in calcified tissue. In rats, IV administration of 0.1 mg/kg [^{14}C]ibandronate showed that ibandronate is rapidly cleared from plasma and that renal excretion is the predominant route of elimination.[8] As with other bisphosphonates, ibandronate is not metabolized, so the radioactivity was entirely accounted for by the intact drug. Radioactivity was 17–38 times higher in calcified versus non-calcified tissue. A total of 40–50% of the dose was found in the entire skeleton, with a terminal elimination half-life of 440–500 days for the trabecular and cortical sections of long bones.[8]

Renal clearance accounts for 50–60% of the elimination of ibandronate from the plasma (54–112 ml/min) and is directly related to creatinine clearance.[19] The remaining ibandronate is absorbed into the bone[19] and slowly clears as it redistributes in the blood. As a result, plasma

elimination is multiphasic, with a half-life of 10–60 h in humans.[19] When administered repeatedly over one year, the concentration of ibandronate in rat bone was found to be linearly related to the systemic dose, suggesting linear kinetics in the dose range tested (0.2–25 μg/kg/day, resulting in a total cumulative dose of approximately 0.07–9.1 mg/kg).[20] Studies in estrogen-depleted rats and dogs indicate that the pharmacodynamic effects of ibandronate on bone is related to the total cumulative dose administered over a given time period and is independent of whether the dose was given daily or less frequently in that period.[20, 21] The pharmacodynamic effects of ibandronate are related to its concentration in bone, which provides the basis for this total dose concept and allows long dose-free treatment intervals.[19,20] In addition to rats and dogs, the efficacy of intermittent treatment with ibandronate on bone mass, strength, architecture and bone turnover has been demonstrated in monkeys and minipigs following estrogen-depletion or chronic corticoid treatment.[22, 23]

Behavioral Analysis

Mice were tested 7, 8, 9, 10, 12 and 14 days following tumor cell or sham inoculation to assess efficacy of ibandronate therapy (100μg/kg, IV at days 7, 8 and 9 post sham or sarcoma injection) in attenuating pain-related behaviors. Animals were observed over a standardized two-minute period each day, during which we characterized the ongoing and palpation-evoked bone cancer pain behaviors, as previously described.[13, 24, 25] Briefly, the number of flinches and time spent guarding the tumor-bearing limb were recorded as measures of ongoing pain, as these measures mirror patients in a clinical setting with bone cancer who protect or suspend their tumor-bearing limb. Movement-evoked pain due to palpation of the injected limb was evaluated using previously validated tests.[17, 25] Palpation-evoked pain behaviors were examined as animals received a normally non-noxious palpation of the tumor cell- or sham-injected limb for two minutes prior to observation.[17] Mice were monitored over a two-minute period, and the number of flinches and time spent guarding were recorded. Palpation-evoked behavior tests were developed to reflect the clinical condition when patients with bone cancer experience increased pain following normally non-noxious movement of the tumor-bearing limb. The ibandronate therapy was compared to acute morphine (Baxter, Deerfield, Illinois; 10mg/kg subcutaneously) treatment and the morphine was administered 15 minutes prior to behavioral testing to ensure that animals were tested within the therapeutic window of drug action.[26]

Euthanasia and Processing of Tissue

Mice were sacrificed at day 10 or 14 post-tumor injection and the tissues were processed for immunohistochemical analysis of spinal cord and femora as previously described.[14, 17, 27, 28] Briefly, mice received a normally non-noxious mechanical stimulation of the injected femur 90 minutes prior to euthanasia for induction of c-Fos expression.[27, 29] Following this manipulation, mice were euthanized with CO_2 and perfused intracardially with 12ml 0.1 M phosphate buffered saline (PBS) followed by 25 ml 4% formaldehyde/12.5% picric acid solution.

Spinal cord segments (L2–L4) were removed, post-fixed in the perfusion fixative overnight and cryoprotected in 30% sucrose at 4° C for 24 hours. Serial frozen spinal cord sections, 60 μm thick, were cut on a sliding microtome, collected in PBS, and processed as free floating sections.

Following sectioning, spinal cord sections were briefly rinsed in PBS and then incubated in blocking solution at 22° C (3% normal donkey serum (NDS) 0.3% Triton X-100 in PBS) for one hr followed by incubation overnight at 22° C in the primary antibody. Spinal cord sections were immunostained for c-Fos protein (1:2,000, Oncogene Research, San Diego, California,

USA) and prodynorphin (polyclonal guinea pig anti-prodynorphin, 1:1,000, Neuromics, Minneapolis, Minnesota, USA).

After incubation in primary antibody solutions, sections were rinsed in PBS three times for 10 minutes each and then incubated in the secondary antibody solution for 3 hours at 22° C. Secondary antibodies, conjugated to Cy3 or biotin (Jackson ImmunoResearch, West Grove, Pennsylvania, USA), were used at 1:600 or 1:500, respectively. In order to detect secondary antibodies conjugated to biotin, following secondary incubation, sections were rinsed in PBS and incubated in Cy3 conjugated streptavidin (1:4000; Jackson ImmunoResearch) for 45 minutes. To confirm specificity of the primary antibodies, controls included omission of the primary antibody or preabsorption with the corresponding synthetic peptide. Following immunostaining procedures, spinal cord sections were mounted onto gelatin-coated slides. All mounted sections were then dehydrated in a successive alcohol gradient scheme (70, 90, 100%), cleared in xylene and coverslipped with DPX (Fluka, Buchs, Switzerland).

Following radiological examination, the animals were perfused at day 10 or day 14 as described above and the right (internal control) and left (tumor-bearing) femora were removed and fixed in picric acid and 4% formalin at 4°C overnight followed by decalcification in 10% EDTA (Sigma., St. Louis, Missouri) for no more than 14 days. Bones were then embedded in paraffin. Femoral sections, 5 mcm thick, were cut in the medial-lateral plane and stained with tartrate-resistant acid phosphatase (TRAP) and hematoxylin and eosin (H&E) to visualize histological features of the normal bone marrow, tumor, osteoclasts and macrophages.

Radiographic Analysis of Tumor-Induced Bone Destruction

Radiographs (Faxitron X-ray Corp., Wheeling, Illinois, USA) of dissected femora were obtained at the day 10 and day 14 time points to assess bone destruction. Images were captured on Kodak Min-R 2000 mammography film (Eastman Kodak Co., Rochester, New York, USA; exposure settings: 7 sec, 21 kVp). The extent of tumor-induced femoral bone destruction was radiologically assessed in the medial-lateral plane of whole bone images at 5X magnification using a 0 to 5 scale (0, normal bone with no signs of destruction and 5, full-thickness bicortical bone loss).[14, 17, 27]

Micro-Computed Tomographic Analysis of Tumor-Induced Bone Destruction

A desktop eXplore Locus SP MicroCT imaging system (GE Healthcare, London, Ontario, Canada) was used to visualize densitometric and architectural parameters in tumorbearing sarcoma + vehicle and sarcoma + ibandronate therapy bones as compared to sham + vehicle bones. The system is equipped with a microfocal X-ray tube providing an 8 um focal spot. The source produces a fan beam that is detected by a charge coupled device (CCD) array with 1024 elements. The specimen is loaded on a turntable that can be shifted automatically in the axial direction. After a data acquisition time set at 300 ms, the turntable with the specimen is rotated by 1° and a new data acquisition process is performed. A standard convolution back projection procedure is used to reconstruct the CT images in 1024×1024 pixel matrices. From the 2D slices obtained, a 3D reconstruction was automatically performed by using a triangulation algorithm.

Analysis of Osteoclasts and Macrophages in Bone

Osteoclast numbers was determined by quantifying the number of TRAP positive osteoclasts at the bone/tumor interface for sarcoma-injected mice and at the normal marrow/bone interface on TRAP stained femoral sections obtained from sham controls as previously described.[14] In brief, osteoclasts are histologically differentiated cells which are TRAP positive, closely associated with regions of bone resorption, multinucleate, and are found in resorption lacunae along the cortical and trabecular bone. Macrophage numbers were determined by quantifying

the number of TRAP positive cells that were freely dispersed throughout the tumor mass and normal hematopoeitic intramedullary space. Macrophages within the bone have been reported to become activated due to tumor released factors that stimulate the cells,[30] and the cellular appearance of these activated macrophages is marked by their highly irregular surface, multiple lamellipodia and phagocytic vacuoles.[31] Results are expressed as the mean number of osteoclasts per mm^2 of intramedullary space or macrophages per mm^2 of intramedullary space.

Quantification of Tumor Growth and Viability

Sections from tumor-bearing femurs were imaged using bright field microscopy on a Olympus BX51 microscope equipped with a Olympus DP70 digital camera utilizing DPController image capture software (Olympus, Melville, New York, USA). The total area of intramedullary space and the percent of intramedullary space occupied by tumor and remaining hematopoeitic cells was calculated using Image Pro Plus v6.0 software (Media Cybernetics, Silver Spring, Maryland, USA). Area of tumor and remaining hematopoeitic cells are presented as a percentage of total intramedullary area.

Quantification of Spinal Cord Immunohistochemistry

Fluorescently-labeled spinal cord tissue sections were analyzed for c-Fos and prodynorphin expression using either an Olympus Fluoview 1000 confocal microscope imaging system or an Olympus DP70 digital camera on an Olympus BX-51 fluorescence microscope with DPController image capture software.

Quantification was carried out in spinal cord sections at lumbar levels L2–L4 as these spinal segments receive significant afferent input from the L1–L5 dorsal root ganglia, which are the principal ganglia that provide afferent input to the mouse femur.[32–35] Quantification of spinal cord sections for prodynorphin was performed on four randomly selected L2–L4 coronal spinal cord sections per animal. The number of prodynorphin-immunoreactive (IR) neurons in spinal cord laminae III–VI were counted at 200x magnification and expressed as mean number of neurons per 60um L2–L4 section per animal. The number of c-Fos-IR neurons was counted in laminae III–VI of the dorsal horn in eight randomly selected L2–L4 coronal spinal cord sections per animal.

Statistical Analysis

The Statview computer statistics package (SAS Institute, Inc., Cary, North Carolina, USA) was used to perform statistical tests. One-way ANOVA was used to compare behavioral results, bone histological results, and immunohistochemical measures among the experimental groups. For multiple comparisons, Fishers's PLSD (protected least significant difference) posthoc test was used. Significance level was set at $P<0.05$. The individual investigator responsible for behavior, immunohistochemical analysis and scoring bone remodeling was blind to the experimental situation of the animal to be analyzed. Results are presented as mean +/− standard error of the mean (SEM).

Results

Ibandronate Therapy Significantly Reduces Bone Cancer Pain-Related Behaviors

Ongoing pain was analyzed by measuring spontaneous guarding and flinching over a two-minute time period. Sarcoma + vehicle mice exhibited significantly greater time spent guarding, as compared to the sham + vehicle controls (Figure 1A). Additionally, sarcoma + vehicle mice exhibited a significant increase in number of flinches as compared to sham + vehicle controls (Figure 1B). Administration of ibandronate (IV, at days 7, 8 and 9) in sarcomainjected mice significantly attenuated spontaneous guarding as compared to sarcoma

+ vehicle mice (Figure 1A). Ibandronate treatment also significantly reduced spontaneous flinching in sarcoma-injected mice (Figure 1B) as compared to sarcoma + vehicle.

Movement-evoked pain was analyzed by measuring palpation-induced responses. Sarcoma + vehicle mice exhibited significantly greater time spent guarding after palpation as compared to the sham + vehicle controls (Figure 1C). Sarcoma + vehicle mice also exhibited a significant increase in number of flinches after palpation as compared to sham + vehicle controls (Figure 1D). Ibandronate treatment in sarcoma-injected mice significantly reduced both palpation-evoked guarding (Figure 1C) and palpation-evoked flinching (Figure 1D). In these studies, no significant side effects, such as ataxia, illness, or lethargy, were observed between animals receiving either vehicle or ibandronate therapy. No significant body weight differences were observed between sarcoma or sham-injected animals or animals receiving either vehicle or ibandronate therapy.

Animals were also tested to compare the efficacy of ibandronate therapy to the acute administration of morphine sulfate (10mg/kg) in reducing bone cancer-related pain behaviors. Behavioral assessment on day 10 revealed that sarcoma + vehicle animals showed statistically significant longer spontaneous time guarding (Figure 1A; 8.5±0.4 sec) and flinching (Figure 1B; 12.7±0.6 flinches), as well as increased time guarding (Figure 1C; 10.2±0.7sec) and flinching (Figure 1D; 15.2±0.7 flinches) in response to palpation of the injected limb as compared to sham + vehicle animals. Treatment with either ibandronate (100μg/kg/day IV given on three consecutive days beginning at day 7) or acute morphine sulfate (10 mg/kg subcutaneously) significantly and to a similar extent reduced both ongoing and movement-evoked guarding and flinching behaviors at day 10 post-tumor injection (Figure 1A, B), as compared to sarcoma + vehicle mice. Sarcoma + ibandronate was significantly different from sham + vehicle for both ongoing and movement-evoked pain behaviors at all time points. The one-time single dose (300μg /kg IV) given as a loading dose was as effective in reducing ongoing and movement-evoked guarding behavior (Figure 1E, F).

Ibandronate Therapy Prevents Bone Destruction and Induces Tumor Cell Necrosis

The effects of ibandronate therapy on bone destruction, osteoclast proliferation, and tumor growth were examined at day 10 and day 14 post-tumor injection. Sham-inoculated vehicle-treated mice did not demonstrate significant bone destruction (bone score 0.6±0.1; Figure 2A) or osteoclast proliferation throughout the entire intramedullary bone/normal marrow interface, including the maintained trabecular regions/marrow interfaces (18±1 osteoclasts/mm^2) (Figure 3A,D), as assessed by radiological, microCT, TRAP and H&E analysis, respectively. In sarcoma + vehicle mice, there was extensive bone destruction, as observed and characterized by multifocal serrated cortical bone radiolucencies and extensive loss of trabecular bone regions in the distal diaphysis (bone score 3.4±0.8; Figure 2B). In addition to osteoclasts along the cortical bone/tumor interface (41±4 osteoclasts/mm^2), the tumor had completely filled the intramedullary space (100±0.0% of intramedullary space; Figure 3B, E). Treatment of sarcoma-injected mice with ibandronate at days 7, 8 and 9 post-tumor inoculation resulted in a significant change in bone resorption (1.7±0.4; Figure 2C), but did not significantly reduce osteoclast proliferation at the bone/tumor interface (36±1 osteoclasts/mm^2) or tumor growth (93.0±0.6% of intramedullary space; Figure 3C, F) as compared to sarcoma + vehicle animals. However, in contrast to vehicle, ibandronate induced extensive tumor cell necrosis in tumor-bearing animals.

At 14 days following tumor injection, sarcoma + vehicle mice displayed a significant number of macrophages (41±8 macrophages/mm^2 intramedullary space) and this number was not significantly different from ibandronate-treated sarcoma-inoculated mice (32±2 macrophages/mm^2 intramedullary space); however both sarcoma + vehicle and sarcoma + ibandronate-

treated animals displayed a significant increase in macrophage infiltration as compared to sham +vehicle inoculated animals (8±1 macrophages/mm^2 intramedullary space) (Table 1).

Using micro-computed tomographic reconstruction, significant visible differences in the degree of osteolytic bone resorption in regions of trabecular bone were apparent at the day 10 endpoint in sham-injected (Figure 2F), sarcoma + vehicle (Figure 2G) and sarcoma + ibandronate-treated animals (Figure 2H): Sarcoma + vehicle animals present extensive trabecular bone resorption, while ibandronate therapy reduce the extent of bone resorption in sarcoma + ibandronate animals such that these femurs closely resembled the features of sham-inoculated controls.

Ibandronate Therapy Prevents Changes Indicative of Neuronal Activation and Central Sensitization in the Spinal Cord

Immediate-early gene activation was attenuated by ibandronate treatment. The expression of c-Fos in the deep dorsal horn (laminae III–VI) has been utilized as a marker of central sensitization in sarcoma-induced bone cancer pain.[14, 17, 36, 37] Normal, non-noxious palpation of sham-operated animals resulted in minimal expression of c-Fos in deep laminae (8.3±2.8; cFos-IR neurons/L3/L4 section; Table 1). Sarcoma + vehicle mice exhibited an increased number of c-Fos immunoreactive (IR) neurons (33.7±7.0; cFos-IR neurons/L3/L4 section; Figure 4A) and treatment with ibandronate significantly prevented this expression (7.2 ±2.4; cFos-IR neurons/L3/L4 section; Figure 4B).

Expression of dynorphin has been shown to be involved in the maintenance of chronic pain.[38, 39] Dynorphin expression has also been shown to be up-regulated in the dorsal horn of the spinal cord in several persistent pain states.[37, 40, 41] In sham + vehicle mice, a small population of spinal neurons expressed the dynorphin precursor peptide, prodynorphin, in deep spinal laminae (2.3±0.6 DYN-IR neurons/L3/L4 section). In contrast, sarcoma + vehicle mice expressed significantly more prodynorphin-IR neurons (4.9±0.6 DYN-IR neurons/L3/L4 section; Figure 4C). Ibandronate treatment significantly prevented the up-regulation of prodynorphin expression (2.3±0.6 DYN-IR neurons/L3/L4 section; Figure 4D) in sarcoma-injected mice.

Discussion

Mechanisms by Which Ibandronate Rapidly Attenuates Bone Cancer Pain

Following confinement and establishment of the tumor in the intramedullary space of the mouse femur, IV administration of the bisphosphonate ibandronate rapidly attenuated ongoing and movement-evoked cancer pain-related behaviors. There are several mechanisms by which ibandronate may inhibit bone cancer pain. First, osteoclasts and tumor cells generate an acidic environment; osteoclasts resorb bone by generating an acidic extracellular microenvironment (pH 4.0 – 5.0) at the osteoclast-mineral interface of bone.[42] The marrow, mineralized bone and periosteum receive extensive innervation by primary afferent sensory neurons [43] and many of these neurons express ion-sensing channels, such as the TRPV1 receptor[44, 45] or the acid-sensing ion channel-3.[46–48] Ibandronate is taken up by osteoclasts that are actively involved in resorption at the bone-nerve interface. Once the osteoclast have a significant concentration of ibandronate within the cell, the mevalonate pathway will be blocked, with resulting loss of the normal activation and localization of GTPases that are involved and required for vesicular trafficking, signal transduction and cytoskeleton function. As all of these are required for the formation of the highly acidic resorption lacunae, the extracellular acidosis that is generated by activated osteoclasts and tumor cells in bone cancer should be attenuated by a reduction of osteoclasts and overall tumor burden, with a resulting decline in the activation of acid sensing ion channels expressed by sensory neurons that innervate the tumor bearing bone.[49, 50]

If ibandronate can reduce the sensitization and activation of nociceptors as described above, ibandronate therapy may also attenuate the central sensitization that may occur in the spinal cord following sustained activation of nociceptors. One marker that is frequently up-regulated with the development of central sensitization in the spinal cord is prodynorphin and this up-regulation is observed as bone cancer pain increases in severity.[37] Previous studies have shown that up-regulation of the pro-hyperalgesic peptide prodynorphin in the spinal cord can be involved in the maintenance of chronic pain, such as that induced by peripheral nerve injury. Thus, cleavage of prodynorphin results in the production of dynorphin, which upon release has been shown to bind to the pro-algesic bradykinin receptors present in the spinal cord.[39, 51–54] Together, these studies suggest that ibandronate treatment not only attenuates tumor-induced activation and injury of sensory fibers in the bone, but also reduces the neurochemical changes in the peripheral and central nervous system that are hypothesized to be involved in generation and maintenance of bone cancer pain.[26]

Ibandronate and Bone Remodeling and Tumor Viability

Within three days of the initial ibandronate administration, there was a significant reduction in tumor-induced bone resorption, as assessed by high resolution x-ray (faxiton), micro-CT and histological analyses. The mechanisms by which ibandronate reduces tumorinduced bone resorption are suggested by previous reports that demonstrate that bisphosphonates inhibit osteoclast recruitment,[55] adhesion,[55–60] and activity.[55, 61] While we did not observe a significant reduction in the total number of osteoclasts, the time points that we examined were only at 4 to 8 days post-administration of ibandronate and does not reflect the clinical situation in human metastatic bone disease, in which long-term treatment (month-years) is the standard.[8] The present observations, which focus primarily on bone pain, are in agreement with previous reports, [62–64] suggesting that the initial effect of administration of a nitrogen-containing bisphosphonate is a reduction in osteoclast activity, with reduction in osteoclast number due to apoptosis being a secondary phenomena that is observed at later time points.[56]

In contrast to long-term studies,[56, 65] short-term administration of ibandronate did not appear to reduce tumor growth, but did result in decreased tumor survival. Thus, at 14 days following injection of tumor cells into the femur the 2472 tumor cells robustly express GFP and show little if any signs of tumor necrosis.[13] In contrast, in animals that had received ibandronate, the tumor cells that filled the intramedullary space began to display histological signs of necrosis. In light of the present and previous studies concerning bisphosphonates' impact on tumor growth,[56, 65] a critical and largely unresolved question is the mechanism(s) by which ibandronate appears to impact tumor growth and viability. Previous reports have suggested that bisphosphonates can have direct tumoricidal actions,[66, 67] influence neovascularization,[68, 69] and have a marked impact on the release of growth factors from bone (by blocking osteoclastmediated bone resorption) that may promote tumor growth and/or survival.[70, 71] While the present results clearly demonstrate that ibandronate can influence tumor viability in the in vivo bone, understanding the specific mechanism(s) by which bisphosphonates reduce tumor growth and/or tumor survival remains an important but unanswered question in tumor and bone biology.

In summary, we have demonstrated, using a single *in vivo* mouse model, that IV ibandronate rapidly attenuates ongoing and movement-evoked bone cancer pain, the neurochemical reorganization of the peripheral and central nervous system, bone destruction and tumor survival. Interestingly, the relief of bone pain afforded by ibandronate was similar to that afforded by acute morphine treatment. Understanding the mechanisms by which bisphosphonates reduce bone pain, tumor growth and tumor-induced skeletal destruction may allow the development of more effective mechanism-based therapies to treat metastatic bone pain as well as the growth and survival of tumor cells that have metastasized to bone.

Acknowledgments

We would like to thank Carl Martin, Juan Miguel Jimenez-Andrade, Christopher Peters, and Therese Schachtele for their commentary and technical assistance during the preparation of this manuscript.

This work was supported by the National Institutes of Health grants (NS23970, NS048021), a Merit Review from the Veterans Administration, and a research grant from Hoffman-La Roche Inc.

References

1. Mercadante S, Arcuri E. Breakthrough pain in cancer patients: pathophysiology and treatment. Cancer Treat Rev 1998;24:425–432. [PubMed: 10189409]
2. Portenoy RK, Hagen NA. Breakthrough pain: definition, prevalence and characteristics. Pain 1990;41:273–281. [PubMed: 1697056]
3. Mercadante S. Malignant bone pain: pathophysiology and treatment. Pain 1997;69:1–18. [PubMed: 9060007]
4. Portenoy RK, Lesage P. Management of cancer pain. Lancet 1999;353:1695–1700. [PubMed: 10335806]
5. Portenoy RK. Managing cancer pain poorly responsive to systemic opioid therapy. Oncology 1999;13:25–29. [PubMed: 10356695]
6. Body JJ. Bisphosphonates for malignancy-related bone disease: current status, future developments. Support Care Cancer 2006;14:408–418. [PubMed: 16450087]
7. Masarachia P, Weinrub M, Balena R, Rodan GA. Comparison of the distribution of 3H-alendronate and 3H-etidronate in rat and mouse bones. Bone 1996;19:281–290. [PubMed: 8873969]
8. Bauss F, Russell RG. Ibandronate in osteoporosis: preclinical data and rationale for intermittent dosing. Osteoporos Int 2004;15:423–433. [PubMed: 15205712]
9. Rogers MJ. New insights into the molecular mechanisms of action of bisphosphonates. Curr Pharm Des 2003;9:2643–2658. [PubMed: 14529538]
10. Rogers MJ, Gordon S, Benford HL, et al. Cellular and molecular mechanisms of action of bisphosphonates. Cancer 2000;88:2961–2978. [PubMed: 10898340]
11. Sato M, Grasser W, Endo N, et al. Bisphosphonate action: alendronate localization in rat bone and effects on osteoclast ultrastructure. J Clin Invest 1991;16:235–245.
12. Heidenreich A, Ohlmann C, Body JJ. Ibandronate in metastatic bone pain. Semin Oncol 2004;31:67–72. [PubMed: 15490379]
13. Sabino MA, Ghilardi JR, Jongen JL, et al. Simultaneous reduction in cancer pain, bone destruction, and tumor growth by selective inhibition of cyclooxygenase-2. Cancer Res 2002;62:7343–7349. [PubMed: 12499278]
14. Honore P, Luger NM, Sabino M, et al. Osteoprotegerin blocks bone cancer-induced skeletal destruction, skeletal pain and pain-related neurochemical reorganization of the spinal cord. Nat Med 2000;6:521–528. [PubMed: 10802707]
15. Sevcik MA, Luger NM, Mach DB, et al. Bone cancer pain: the effects of the bisphosphonate alendronate on pain, skeletal remodeling, tumor growth and tumor necrosis. Pain 2004;111:169–180. [PubMed: 15327821]
16. Sevcik MA, Ghilardi JR, Peters CM, et al. Anti-NGF therapy profoundly reduces bone cancer pain and the accompanying increase in markers of peripheral and central sensitization. Pain 2005;115:128–141. [PubMed: 15836976]
17. Luger NM, Honore P, Sabino MAC, et al. Osteoprotegerin diminishes advanced bone cancer pain. Cancer Res 2001;61:4038–4047. [PubMed: 11358823]
18. Muhlbauer RC, Bauss F, Schenk R, et al. BM 21.0955, a potent new bisphosphonate to inhibit bone resorption. J Bone Miner Res 1991;6:1003–1011. [PubMed: 1838661]
19. Barrett J, Worth E, Bauss F, et al. Ibandronate: a clinical pharmacological and pharmacokinetic update. J Clin Pharmacol 2004;44:951–965. [PubMed: 15317823]

20. Bauss F, Lalla S, Endele R, et al. Effects of treatment with ibandronate on bone mass, architecture, biomechanical properties, and bone concentration of ibandronate in ovariectomized aged rats. J Rheumatol 2002;29:2200–2208. [PubMed: 12375334]
21. Monier-Faugere MC, Geng Z, Paschalis EP, et al. Intermittent and continuous administration of the bisphosphonate ibandronate in ovariohysterectomized beagle dogs: effects on bone morphometry and mineral properties. J Bone Miner Res 1999;14:1768–1778. [PubMed: 10491225]
22. Smith SY, Recker RR, Hannan M, et al. Intermittent intravenous administration of the bisphosphonate ibandronate prevents bone loss and maintains bone strength and quality in ovariectomized cynomolgus monkeys. Bone 2003;32:45–55. [PubMed: 12584035]
23. Gluer CC, Scholz-Ahrens KE, Helfenstein A, et al. Ibandronate treatment reverses glucocorticoid-induced loss of bone mineral density and strength in minipigs. Bone 2007;40:645–655. [PubMed: 17174621]
24. Luger NM, Sabino MA, Schwei MJ, et al. Efficacy of systemic morphine suggests a fundamental difference in the mechanisms that generate bone cancer vs inflammatory pain. Pain 2002;99:397–406. [PubMed: 12406514]
25. Sabino MA, Luger NM, Mach DB, et al. Different tumors in bone each give rise to a distinct pattern of skeletal destruction, bone cancer-related pain behaviors and neurochemical changes in the central nervous system. Int J Cancer 2003;104:550–558. [PubMed: 12594809]
26. Hasselstrom J, Svensson JO, Sawe J, et al. Disposition and analgesic effects of systemic morphine, morphine-6-glucuronide and normorphine in rat. Pharmacol Toxicol 1996;79:40–46. [PubMed: 8841095]
27. Honore P, Rogers SD, Schwei MJ, et al. Murine models of inflammatory, neuropathic and cancer pain each generates a unique set of neurochemical changes in the spinal cord and sensory neurons. Neuroscience 2000;98:585–598. [PubMed: 10869852]
28. McCarty BG, Hsieh ST, Stocks A, Hauer P, et al. Cutaneous innervation in sensory neuropathies: evaluation by skin biopsy. neurology 1995;45:1848–1855. [PubMed: 7477980]
29. Hunt SP, Pini A, Evan G. Induction of c-fos-like protein in spinal cord neurons following sensory stimulation. Nature 1987;328:632–634. [PubMed: 3112583]
30. Orr FW, Sanchez-Sweatman OH, Kostenuik P, et al. Tumor-bone interactions in skeletal metastasis. Clin Orthop Relat Res 1995:19–33. [PubMed: 7634602]
31. McBride WH. Phenotype and functions of intratumoral macrophages. Biochimica et Biophysica Acta 1986;865:27–41. [PubMed: 3524684]
32. Edoff K, Grenegard M, Hildebrand C. Retrograde tracing and neuropeptide immunohistochemistry of sensory neurones projecting to the cartilaginous distal femoral epiphysis of young rats. Cell Tissue Res 2000;299:193–200. [PubMed: 10741460]
33. Molander C, Grant G. Spinal cord projections from hindlimb muscle nerves in the rat studied by transganglionic transport of horseradish peroxidase, wheat germ agglutinin conjugated horseradish peroxidase, or horseradish peroxidase with dimethylsulfoxide. J Comp Neurol 1987;260:246–255. [PubMed: 3038969]
34. Puigdellivol-Sanchez A, Forcada-Calvet P, Prats-Galino A, Molander C. Contribution of femoral and proximal sciatic nerve branches to the sensory innervation of hindlimb digits in the rat. Anat Rec 2000;260:180–188. [PubMed: 10993954]
35. Puigdellivol-Sanchez A, Prats-Galino A, Ruano-Gil D, Molander C. Sciatic and femoral nerve sensory neurones occupy different regions of the L4 dorsal root ganglion in the adult rat. Neurosci Lett 1998;251:169–172. [PubMed: 9726370]
36. Honore P, Schwei MJ, Rogers SD, et al. Cellular and neurochemical remodeling of the spinal cord in bone cancer pain. Prog Brain Res 2000;129:389–397. [PubMed: 11098706]
37. Schwei MJ, Honore P, Rogers SD, et al. Neurochemical and cellular reorganization of the spinal cord in a murine model of bone cancer pain. J Neurosci 1999;19:10886–10897. [PubMed: 10594070]
38. Vanderah TW, Ossipov MH, Lai J, et al. Mechanisms of opioid-induced pain and antinociceptive tolerance: descending facilitation and spinal dynorphin. Pain 2001;92:5–9. [PubMed: 11323121]
39. Vanderah TW, Laughlin T, Lashbrook JM, et al. Single intrathecal injections of dynorphin A or des-Tyr-dynorphins produce long-lasting allodynia in rats: blockade by MK-801 but not naloxone. Pain 1996;68:275–281. [PubMed: 9121815]

40. Iadarola MJ, Douglass J, Civelli O, et al. Differential activation of spinal cord dynorphin and enkephalin neurons during hyperalgesia: evidence using cDNA hybridization. Brain Res 1988;455:205–212. [PubMed: 2900057]
41. Noguchi K, Kowalski K, Traub R, et al. Dynorphin expression and Fos-like immunoreactivity following inflammation induced hyperalgesia are colocalized in spinal cord neurons. Mol Brain Res 1991;10:227–233. [PubMed: 1679515]
42. Delaisse, J-M.; Vaes, G. Mechanism of mineral solubilization and matrix degradation in osteoclastic bone resorption. In: Rifkin, BR.; Gay, CV., editors. Biology and physiology of the osteoclast. CRC; Ann Arbor: 1992. p. 289-314.
43. Mach DB, Rogers SD, Sabino MC, et al. Origins of skeletal pain: sensory and sympathetic innervation of the mouse femur. Neuroscience 2002;113:155–166. [PubMed: 12123694]
44. Caterina MJ, Schumacher MA, Tominaga M, et al. The capsaicin receptor: a heat-activated ion channel in the pain pathway. Nature 1997;389:816–824. [PubMed: 9349813]
45. Tominaga M, Caterina MJ, Malmberg AB, et al. The cloned capsaicin receptor integrates multiple pain-producing stimuli. Neuron 1998;21:531–543. [PubMed: 9768840]
46. Bassilana F, Champigny G, Waldmann R, et al. The acid-sensitive ionic channel subunit ASIC and the mammalian degenerin MDEG form a heteromultimeric H+-gated Na+ channel with novel properties. J Biol Chem 1997;272:28819–28822. [PubMed: 9360943]
47. Olson TH, Riedl MS, Vulchanova L, et al. An acid sensing ion channel (ASIC) localizes to small primary afferent neurons in rats. Neuroreport 1998;9:1109–1113. [PubMed: 9601677]
48. Waldmann R, Champigny G, Bassilana F, et al. A proton-gated cation channel involved in acid-sensing. Nature 1997;386:173–177. [PubMed: 9062189]
49. Luckman S, Hughes D, Coxon F, et al. Nitrogen-containing bisphosphonates inhibit the mevalonate pathway and prevent post-translational prenylation of GTP-binding proteins, including Ras. J Bone Miner Res 1998;13:581–584. [PubMed: 9556058]
50. Wakchoure S, Merrell MA, Aldrich W, et al. Bisphosphonates inhibit the growth of mesothelioma cells in vitro and in vivo. Clin Cancer Res 2006;12:2862–2868. [PubMed: 16675582]
51. Lai J, Luo MC, Chen Q, et al. Dynorphin A activates bradykinin receptors to maintain neuropathic pain. Nat Neurosci 2006;9:1534–1540. [PubMed: 17115041]
52. Malan TP, Ossipov MH, Gardell LR, et al. Extraterritorial neuropathic pain correlates with multisegmental elevation of spinal dynorphin in nerve-injured rats. Pain 2000;86:185–194. [PubMed: 10779675]
53. Ossipov MH, Lai J, Malan TP Jr, et al. Spinal and supraspinal mechanisms of neuropathic pain. Ann N Y Acad Sci 2000;909:12–24. [PubMed: 10911921]
54. Wang Z, Gardell L, Ossipov M, et al. Pronociceptive actions of dynorphin maintain chronic neuropathic pain. J Neurosci 2001;21:1779–1786. [PubMed: 11222667]
55. Vasikaran V. Bisphosphonates: an overview with special reference to alendronate. Ann Clin Biochem 2001;38:608–623. [PubMed: 11732644]
56. Hiraga T, Williams PJ, Mundy GR, et al. The bisphosphonate ibandronate promotes apoptosis in MDA-MB-231 human breast cancer cells in bone metastases. Cancer Res 2001;61:4418–4424. [PubMed: 11389070]
57. Virtanen S, Vaananen HK, Harkonen P, Lakkakorpi P. Alendronate inhibits invasion of the PC-3 prostate cancer cells by affecting the mevalonate pathway. Cancer Res 2002;62:2708–2714. [PubMed: 11980672]
58. Shipman C, Croucher P, Russell R, et al. The bisphosphonate incadronate (YM175) causes apoptosis of human myeloma cells in vitro by inhibiting the mevalonate pathway. Cancer Res 1998;58:5294–5297. [PubMed: 9850051]
59. Fromigue O, Lagneaux L, Body JJ. Bisphosphonates induce breast cancer cell death in vitro. J Bone Miner Res 2000;15:2211–2221. [PubMed: 11092402]
60. Neville-Webbe HL, Coleman RE. The use of zoledronic acid in the management of metastatic bone disease and hypercalcaemia. Palliat Med 2003;17:539–553. [PubMed: 14526888]
61. Toyras AOJ, Taskinen M, Monkkonen J. Inhibition of the mevalonate pathway is involved in alendronate-induced cell growth inhibition, but not in cytokine secretion from macrophages in vitro. Eur J Pharm Sci 2003;19:223–230. [PubMed: 12885386]

62. Breuil V, Cosman F, Stein L, et al. Human osteoclast formation and activity in vitro: effects of alendronate. J Bone Miner Res 1998;13:1721–1729. [PubMed: 9797481]

63. Boissier S, Ferreras M, Peyruchaud O, et al. Bisphosphonates inhibit breast and prostate carcinoma cell invasion, an early event in the formation of bone metastases. Cancer Res 2000;60:2949–2954. [PubMed: 10850442]

64. Alakangas A, Selander K, Mulari M, et al. Alendronate disturbs vesicular trafficking in osteoclasts. Calcif Tissue Int 2002;70:40–47. [PubMed: 11907706]

65. Neudert M, Fischer C, Krempien B, et al. Site-specific human breast cancer (MDA-MB-231) metastases in nude rats: model characterisation and in vivo effects of ibandronate on tumour growth. Int J Cancer 2003;107:468–477. [PubMed: 14506749]

66. Lipton A, Theriault RL, Hortobagyi GN, et al. Pamidronate prevents skeletal complications and is effective palliative treatment in women with breast carcinoma and osteolytic bone metastases: long term follow-up of two randomized, placebo-controlled trials. Cancer 2000;88:1082–1090. [PubMed: 10699899]

67. Walker K, Medhurst SJ, Kidd B, Glatt M, et al. Disease modifying and anti-nociceptive effects of the bisphosphonate, zoledronic acid in a model of bone cancer pain. Pain 2002;100:219–229. [PubMed: 12467993]

68. Fournier P, Boissier S, Filleur S, et al. Bisphosphonates inhibit angiogenesis in vitro and testosterone-stimulated vascular regrowth in the ventral prostate in castrated rats. Cancer Res 2002;62:6538–6544. [PubMed: 12438248]

69. Wood J, Bonjean K, Ruetz S, et al. Novel antiangiogenic effects of the bisphosphonate compound zoledronic acid. J Pharmacol Exp Ther 2002;302:1055–1061. [PubMed: 12183663]

70. Hughes DE, MacDonald BR, Russell RG, et al. Inhibition of osteoclast-like cell formation by bisphosphonates in long-term cultures of human bone marrow. J Clin Invest 1989;83:1930–1935. [PubMed: 2524504]

71. Sato M, Grasser W. Effects of bisphosphonates on isolated rat osteoclasts as examined by reflected light microscopy. J Bone Miner Res 1990;5:31–40. [PubMed: 2106763]

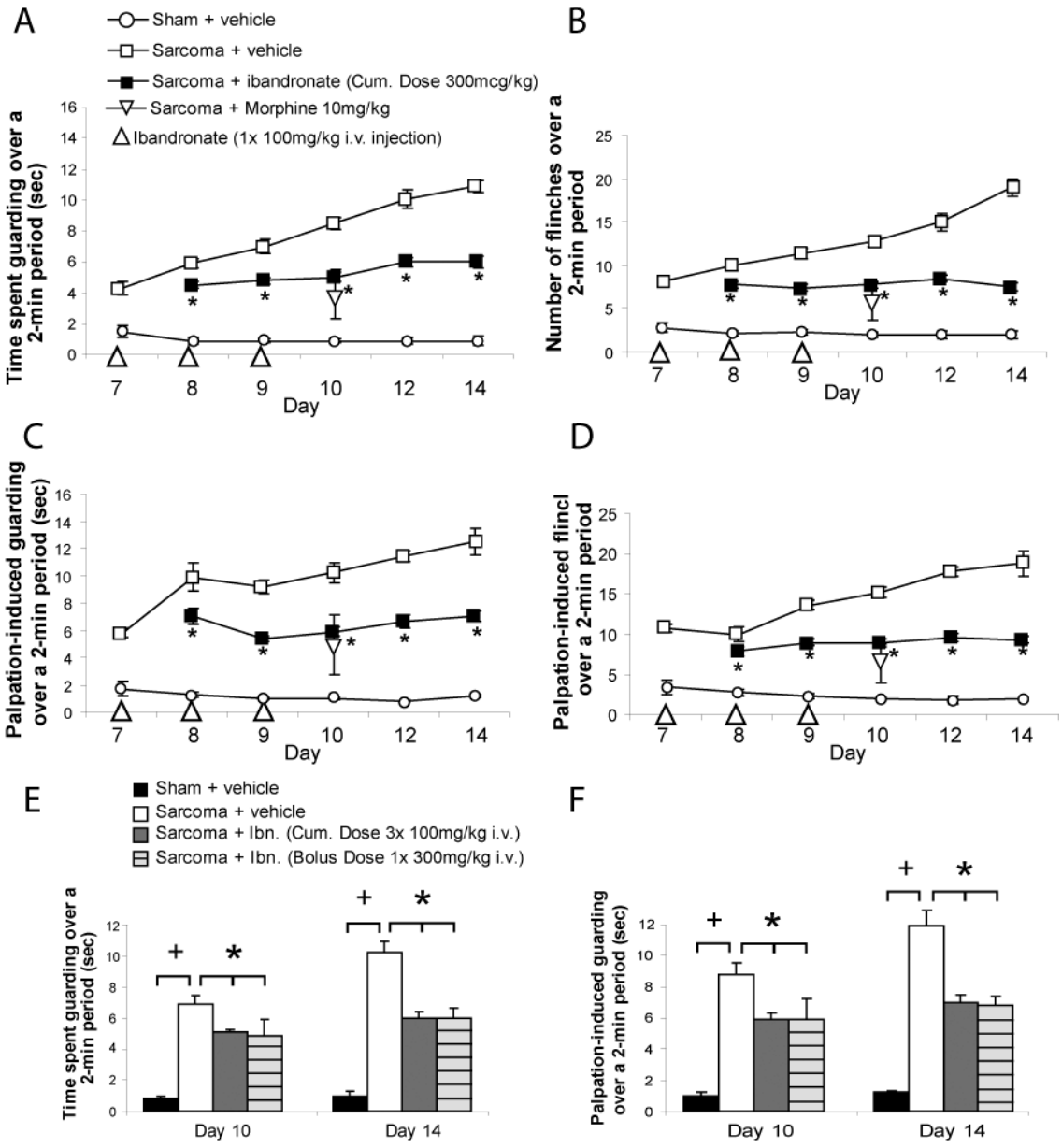

Figure 1.

Ibandronate therapy attenuates bone cancer pain-related behaviors. Ibandronate treatment (100 μg/kg at days 7, 8 and 9 post sham or sarcoma injection, IV) attenuated both ongoing and movement-evoked bone cancer pain behaviors throughout the progression of the disease. The time spent guarding and number of spontaneous flinches of the sarcoma injected limb over a 2-minute observation period was used as a measure of ongoing pain. This standardized 2-minute observation of the animals behavior was performed at 7, 8, 9, 10, 12 and 14 days post sham or sarcoma injection (A,B). Parameters of movement-evoked pain included quantification of time spent guarding and the number of flinches over a 2-minute observation period following a normally non-noxious palpation of the sham or sarcoma-injected femur (C, D). Note that ibandronate treatment (large triangle at days 7, 8 and 9) post-tumor injection (closed square) significantly reduced ongoing and palpation-evoked pain behaviors on days 8, 9, 10, 12 and 14 as compared to sarcoma + vehicle (open square). Acute morphine sulfate

(small open triangle; 10 mg/kg subcutaneously) also significantly reduced both ongoing and movement-evoked guarding and flinching behaviors at day 10 post-tumor injection (Figure 1A, B), as compared to sarcoma + vehicle mice. At 7, 8, 9, 10, 12 and 14 days post injection, sham + vehicle (open circle) are significantly different from sarcoma + vehicle. Note that a one-time single dose (300μg/kg IV) was as effective as a loading dose in reducing ongoing (E) and movement-evoked (F) guarding behavior. Sarcoma + ibandronate was significantly different from sham + vehicle for ongoing and movement-evoked pain behaviors at all time points. Error bars represent S.E.M. * = $P<0.05$ vs. sarcoma + vehicle; + = $P<0.05$ vs. sham + vehicle.

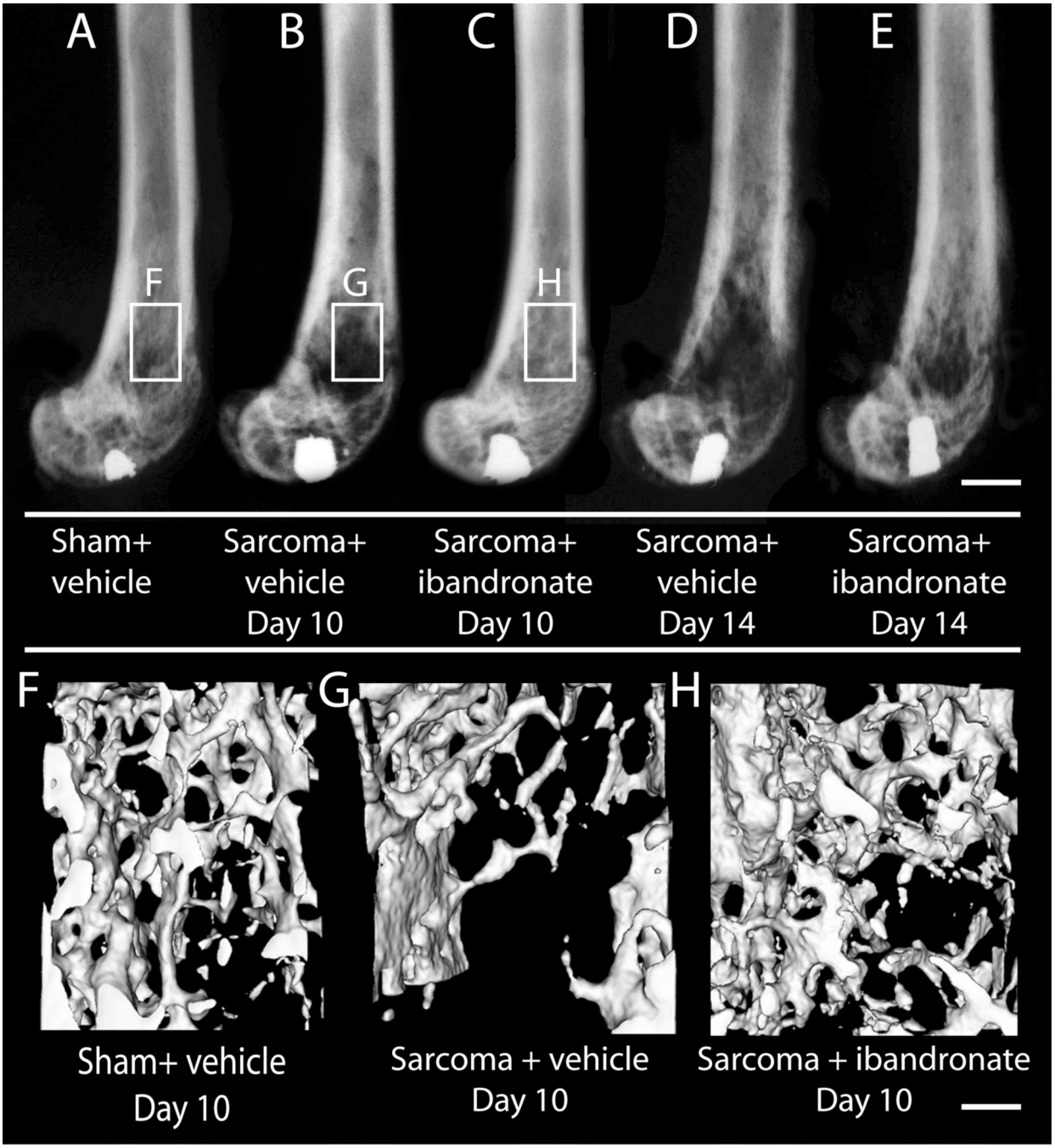

Figure 2.

Ibandronate therapy has a significant effect on reducing tumor-induced bone destruction at day 10 and day 14 post-tumor injection as assessed by high-resolution faxitron analysis. Sham animals, (A) show no radiographically apparent bone destruction at day 10, whereas sarcoma + vehicle (B) animals show a transition from the radio-opaque bone tissue to a radio-lucent appearance by day 10. Sarcoma + ibandronate (C) animals present a markedly reduced pattern and extent of bone destruction as sarcoma + vehicle animals. Sham-injected mouse femurs (F) present a net maintenance of trabecular bone while 2472 sarcoma-injected femurs (G) display osteolytic resorption of trabecular structure at the distal diaphysis of the femur when analyzed with microCT imaging at day 10 post-tumor injection. Treatment with ibandronate

significantly attenuates the loss of trabecular bone when viewed with microCT imaging (G) at day 10 post-tumor injection. Scale bars: A–H; .4mm. **AU: .4 OR 4?**

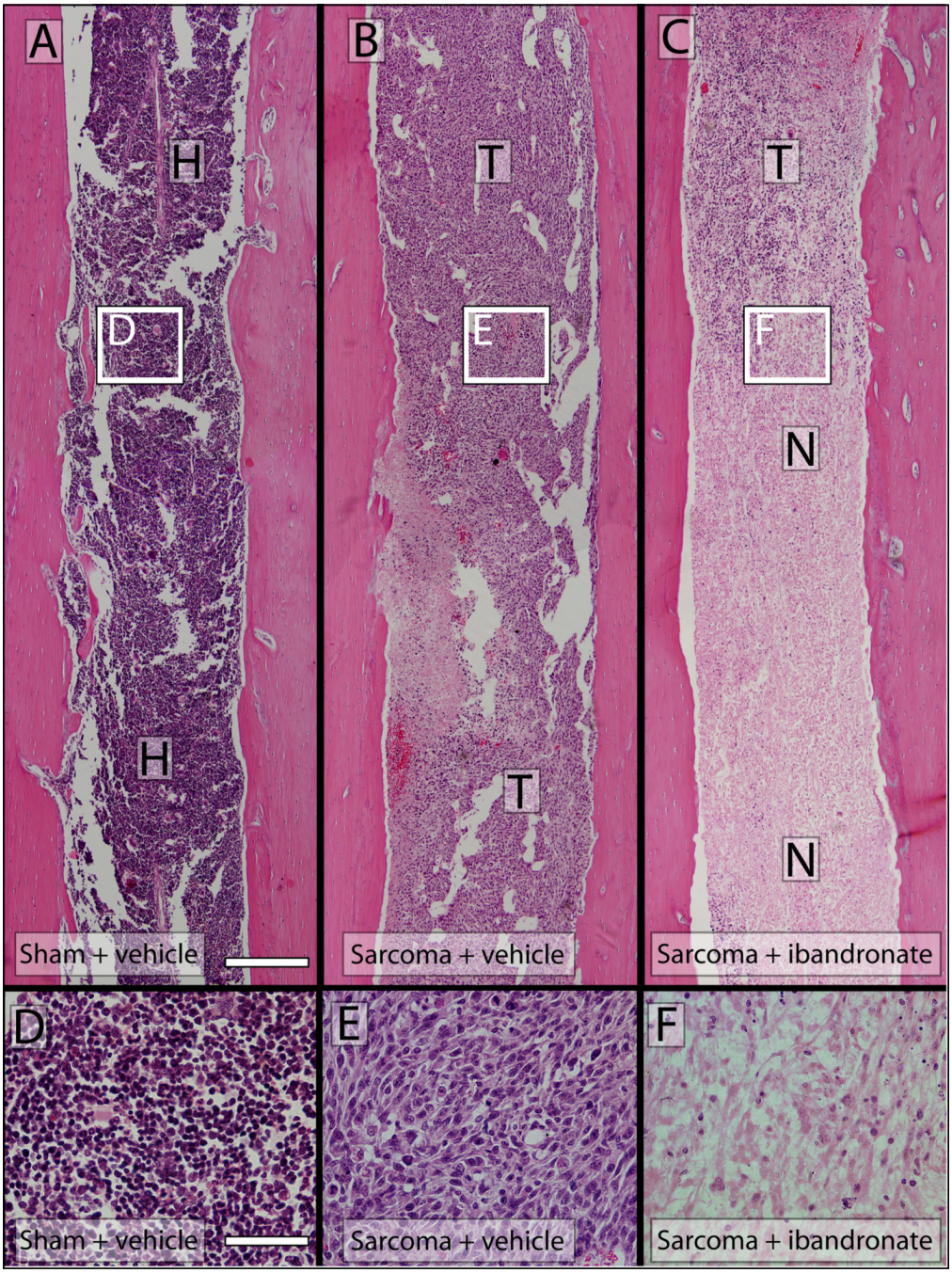

Figure 3.

Hematoxylin and eosin-stained histological comparison of tumor burden and necrosis in sham, sarcoma + vehicle and sarcoma + ibandronate treated femurs day 14 post-tumor injection. Sham-injected mouse femurs (A) present neither visibly detectable newly formed bone or bone destruction when assessed after hematoxylin and eosin staining (H&E). 2472 sarcomainjected femurs display primarily osteolytic characteristics and replacement of the intramedullary space with tumor cells and limited necrosis (B) where tumor cell apoptosis has occurred. Sarcoma + ibandronate femurs present complete replacement of the intramedullary space with tumor cells and extensive necrosis of the tumor mass at day 14 post-injection. High power images of sham

(D), sarcoma + vehicle (E) and sarcoma + ibandronate (F) intramedullary space. A–C; Scale bar = 4mm, D–F; Scale bar = 0.25mm. T= tumor; H= hematopoeitic cells; N= necrosis.

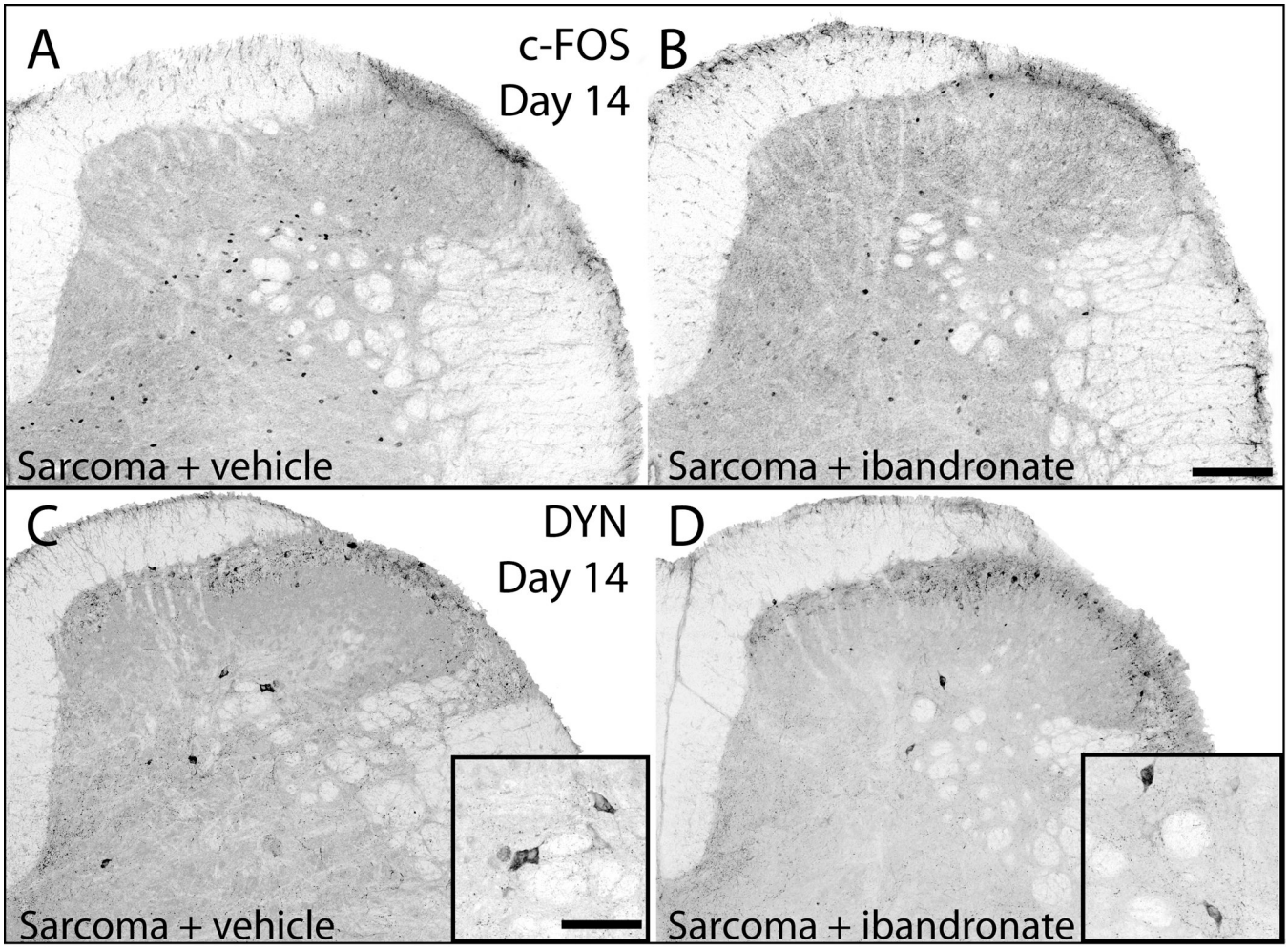

Figure 4.

Neurochemical changes associated with central sensitization are attenuated by administration of ibandronate. Representative confocal images of c-Fos expressing neurons of the spinal cord in sarcoma + vehicle (A) and sarcoma + ibandronate (B) mice. Following a normally non-noxious palpation of tumor-bearing limbs, sarcoma + vehicle mice showed an increased expression of c-Fos protein in neurons within the deep laminae. In sarcoma animals that received ibandronate therapy, there was a significant reduction of this increased expression of c-Fos protein. Representative confocal images of prodynorphin expression (DYN) in the dorsal horn of the spinal cord in sarcoma + vehicle (C) and sarcoma + ibandronate (D) mice. Sarcoma + vehicle mice displayed an increase in prodynorphin-IR neurons in deep laminae of the ipsilateral spinal cord (C), whereas ibandronate therapy significantly attenuated the increase in prodynorphin expression (D). Scale bar: A, B 150mcm; insets in C,D 200mcm.

Table 1

Histological & Immunohistochemical qualification of bone remodeling, tumor progression, and neurochemical changes in ibandronate (3 × 100μg/kg cum.) and 2472 + Vehicle treated Mice

	Sham + Vehicle	2472 + Vehicle	2472 + Ibanreonate
1. Bone Histomorphometry (Day 14)			
Osteoclasts (OC # throughout the intramedullary space)	193±4	**345±70**[a]	**323±14**[a]
Macrophages (Ms # throughout the intramedullary space)	19±2	**77±7**[a]	**68±2**[a]
Tumor cells (% intramedullary space occupied)	0±0	**100±0**[a]	**93±6**[a]
Hematopoetic Cells (% intramedullary space occupied)	100±0	**0±0**[a]	**7±4**[a]
2. Immunohistochemistry (Day 14)			
Spinal Cord			
c-Fos (LIII–VI)	8.5±2.8	**33±7**[a,b]	**7.2±2.4**[a,b]
Dynorphin (LIII–VI)	2.3±0.6	**4.9±0.6**[a,b]	**2.3±0.6**[a,b]
Gilal Fibrillary Acidic Protein (GFAP) Expressed as % of Sham Value	100±11	126±48	112±7

[a] $P<0.005$ versus sham + vehicle (one way ANOVA, Fisher's PLSD).

[b] $P<0.005$ versus 2472 + vehicle (one way ANOVA, Fisher's PLSD).